# Provenance study of Phanerozoic rocks from the Cordillera Real of Bolivia

Alvaro Rodrigo Iriarte[1,2]* , Umberto Giuseppe Cordani[1] , Miguel Basei[1]

## Abstract

U/Pb ages of detrital zircon from two samples of Ordovician sediments were determined and, based on similar published data, were compared with xenocrystal inheritance of Triassic and Oligocene granitoids of the Cordillera Real in order to better understand their genetic relationship and sources. The results show that the detrital zircon in the Ordovician sandstone and the inherited zircon cores in granitoids are statistically correlated. This correlation suggests assimilation of these sedimentary units by the felsic melts. Ages ranging from 300 to 2300 Ma are recorded in these inherited zircons. A high peak of Cambrian to late Neoproterozoic ages (500–750 Ma) is observed throughout metasedimentary units of the entire belt. Candidates for the main sources of these zircons include: Brasiliano or Pampean belts and/or an "in situ" hidden belt within the Central Andes or via recycling of detrital zircons in pre-existing sedimentary rocks. It is also possible that the sources lie below modern sedimentary covers but, at the time, formed high relief structures supplying recycled material into the Ordovician basins.

**KEYWORDS:** U/Pb zircon dating; Central Andes; granitoids; Ordovician sediments.

## INTRODUCTION

The dating of sedimentary sequences has been improved over the last decades thanks to the use of mass spectrometers capable of analyzing large numbers of mineral samples, so that the ages of stratigraphic units can be better understood. Mass spectrometers used to date zircon and other key minerals are Sensitive High-Resolution Ion Micro Probe (SHRIMP) (secondary ionization) and Laser Ablation Inductively Coupled Plasma Mass Spectrometry (LA-ICP-MS) (laser excitation). The latter is more extensively used in provenance studies, because of the relatively low cost and rapid results.

The Central Andes, from southern Peru to northern Chile, are cored by an orogenic belt along the western border of South America. It is mostly characterized by Phanerozoic sedimentary and metamorphic sequences intruded by Paleozoic to Recent granitoids. Several regional studies have shown a complex history through geological time, consisting of terrane amalgamation, mobile belt tectonism, mountain building, erosion, and recycling (Franz *et al*. 2006, Jiménez and López-Velásquez

2008, Ramos 2018). U/Pb zircon ages and geochemical signatures reflect these processes. In this sense, it has been shown that most sources of detrital materials are located in neighboring eastern Amazonia (Reimann *et al*. 2010; Calle *et al*. 2017, Vasconcelos 2018).

For the case of the Cordillera Real of Bolivia, Triassic granitic intrusive magmas interacted with pre-existing sedimentary sequences. As shown by field evidence and isotopic signature (Cordani *et al*. 2019), processes such as AFC (assimilation and crystal fractionation, DePaolo 1981) can be easily envisioned as plausible during emplacement.

Analyses of U/Pb ages recorded (and conserved) in zircon crystals of granites and their country rocks have been very useful to understand "hidden" basement rocks below the surface, which are the potential sources for these granitic melts (e.g., the Lachlan fold belt, Keay *et al*. 1999).

The objectives of this paper are: to compare the U/Pb ages of detrital zircons of early-Paleozoic sedimentary country rocks with those of xenocrystal zircon crystals from the granitoids of the Cordillera Real in order to better understand the genetic relationship between granites and their sedimentary envelope; and to picture the potential paleo-relief in South America during Triassic times, and envisage potential source areas of detrital zircon grains.

## GEOLOGICAL BACKGROUND

The Cordillera Real granitoids (CRG) are a group of upper crustal plutons emplaced at ca. 220 Ma, with a younger pulse at ca. 27 Ma (Gillis *et al*. 2006, Cordani *et al*. 2019, Iriarte *et al*. 2021). Their country rocks have early Paleozoic ages (Fig. 1) and

---

[1]Universidade de São Paulo – São Paulo (SP), Brazil. E-mails: arodrigoiriarte@usp.br, ucordani@usp.br, baseimas@usp.br

[2]Universidad Mayor de San Andrés – La Paz, Bolivia.

*Corresponding author.

continue towards SE Peru. There, Kontak *et al.* (1990) described the intrusive suite of the Carabaya Cordillera, as a complex suite of felsic and mafic magmatic units. Regionally, this magmatism corresponds to the Gondwanide Orogeny (336–200 Ma, Ramos 2018), characterized by an overall subduction system, which was synchronous at 240 Ma with a regional continental rift.

## Cordillera Real Granitoids

The CRGs are a suite of sub-circular to elliptical plutons, emplaced along the NW strike axis of the Eastern Cordillera (Fig. 1). They are composed of quartz-diorites, monzonites, granodiorites, and two mica granites with calc-alkaline within plate affinities, some being peraluminous.
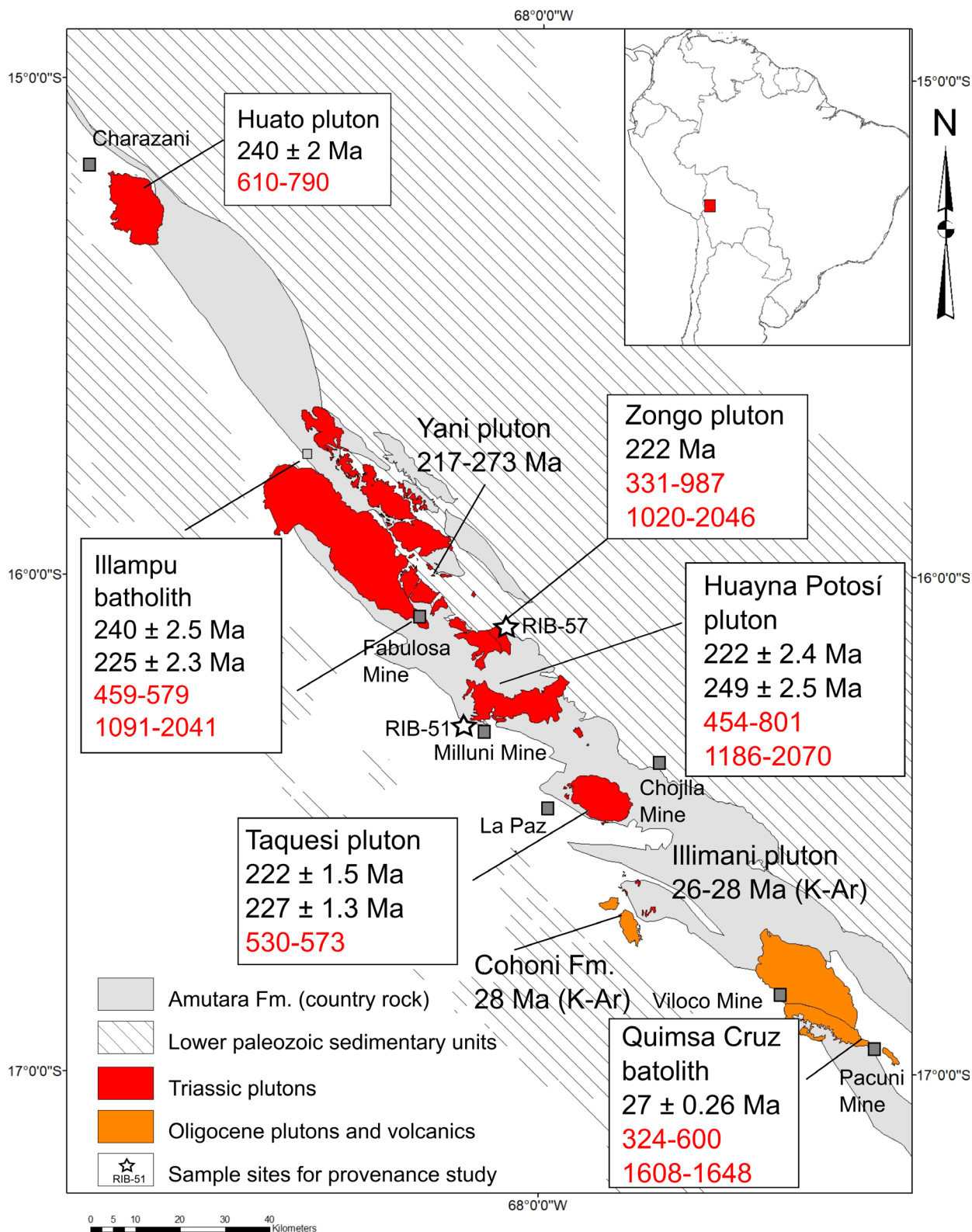


Source: modified from published maps of the Geological Service of Bolivia (GEOBOL 1994, 1995, 1997, 2013).
**Figure 1.** Cordillera Real granitoids (CRGs) showing their U/Pb crystallization ages (in black) and age ranges of inherited xenocrystal zircons (in red). The country rock is mostly represented by the Amutara Fm.

U/Pb SHRIMP dating (Gillis *et al.* 2006, Iriarte *et al.* 2021) revealed a protracted history of magmatism of nearly 60 Ma, starting at ca. 280 and ending at ca. 220 Ma. Quartz diorites and tonalites were emplaced at the beginning of the continental rift (~280 Ma). Magmas "evolved" via an AFC process towards more calc-alkaline compositions, during final pluton crystallization at 220 Ma.

Because of the relatively low zircon saturation temperatures, oversaturation, and, therefore, better preservation of inheritance and assimilated wall rock material, zircon antecrysts and xenocrysts were conserved (Tab. 1 and Fig. 1, Iriarte *et al.* 2021). Ages of inherited zircons range from ca. 330 Ma (initiation of the Gondwanide orogeny) to ca. 2300 Ma. Most are inherited cores surrounded by younger overgrowths (Cordani *et al.* 2019). As the country rocks are early Paleozoic sediments, most xenocrysts were probably derived from these stratigraphic units during the emplacement of S-like granites (Ávila 1990).

Figure 1 shows that, except for the Oligocene Quimsa Cruz pluton, all the others are Triassic in age. The distance between the Huato pluton in the NW and the Quimsa Cruz pluton in the SE is about 250 Km. Moreover, Figure 1 shows that all plutons cut through the entire thickness of the Amutara Formation, of the order of several hundred meters, as well as through the sedimentary pile underneath, belonging to the Eastern Andes. To check the possibility that the xenocrysts encountered in the Cordillera Real plutons could be grains inherited from these sedimentary rocks, we tried to compare them with the detrital grains included in the Ordovician sediments.

Table 1 shows that a total of 64 zircon xenocrysts was recovered from the plutons studied by Iriarte *et al.* (2021). Twelve of them are younger than the Ordovician Amutara Formation and, therefore, must be considered as grains ultimately inherited from igneous intrusions related to the Famatinian or Gondwanan magmatic rocks. It is also possible that these detrital zircons came from sedimentary sources bearing older xenocrysts (> ca. 480 Ma).

These 44 zircon crystals, with U-Pb SHRIMP Precambrian or Cambrian ages, most likely originated as detrital grains within the Ordovician units. Many of these zircon grains were scattered in the Zongo (17) and Huayna Potosi (15) plutons, located not far from the location of RIB-51 and RIB-57 samples (see Figure 1). The remaining 12 grains were from the Huato (2), Illampu (5) Taquesi (2), and Quimsa Cruz (3) plutons. Assuming that these xenocrysts were indeed previous detrital zircon crystals belonging to the country rocks, to achieve a better statistical representation, all pre-Ordovician ages were grouped as composite sample CRG.

## Stratigraphy of Ordovician country rocks

Ordovician sedimentary units are widespread along the Central Andes, including the Altiplano, the Western and Eastern cordilleras. Locally, they belong to the Tacsarian Cycle, which includes Cambrian and Ordovician sedimentary sequences (Suárez-Soruco 1992).

The oldest outcropping unit of the area of study is the Coroico Formation (Suárez-Soruco 1992) a thick metapelite sequence of shales and mudstones deposited in a deep marine shelf. It grades upwards to coarser grain size banks. Fossil fauna suggests a Llanvirnian age (~470 Ma). The passage from the Coroico Formation to the upper Amutara Formation is transitional.

The Tacsarian Cycle ends in the northern Eastern Cordillera with an alternation of sandstones, and mudstones of hundreds of meters thick. These rocks are considered to be Upper Ordovician in age and were designated as the Amutara Formation (Fig. 1, Voges 1962). They were deposited in a marine shelf within a foreland basin. Fossil fauna suggests a Sandbian age (~458 Ma).

## Sample site description

We took samples from two sedimentary units near the contact with plutons representative of the CRG for our study of provenance and then we compared our results with results related to sedimentary units from published data.

Sample RIB-51 was taken from the NE flank of a small anticline at the SW border of the Huayna Potosí granite (S16º17'36.33", W68º7'56.61", Fig. 1). It is characterized by 5 to 10 cm thick laminated banks of sandstone affected by the veining of iron oxides. It strikes N136ºW dipping 53º NE. A thin section analysis shows rounded clasts of quartz (74%), muscovite (10%), and a matrix made mostly of clays (10%), minor tourmaline (< 1%), (30 to 100 µm) rounded zircon, and iron oxides.

Sample RIB- 57 was taken from a sequence of schists cropping out at the NE border of the Zongo granite (S16º6'17.84", W68º3'58.69", Fig. 1). It is characterized by porphyroblasts of andalusite (up to 5 cm in length) surrounded by a matrix of micas and quartz. It strikes N170ºS dipping 65º NE. A thin section analysis shows rounded porphyroblasts of quartz (20%), andalusite (15%), biotite (18%), muscovite (10%), clastic matrix (30%), tourmaline (2%), minor amounts (< 1%) of anhedral zircon (10 to 100 µm), apatite, and iron oxides.

## METHODOLOGY: LA-ICP-MS ANALYSES

Sample preparation, cathodoluminescence imaging (CL), and geochronological analyses were carried out at Centro de Pesquisas Geocronológicas, at Universidade de São Paulo, Instituto de Geociências. Zircon crystals were extracted from crushed and sieved rocks using magnetic and heavy liquid separation methods. Hand-picked crystals from each sample were arranged in rows, cast into epoxy resin discs, and polished to reveal grain internal structures. The reference standard used to calibrate the measured U/Pb ratios was GJ-1 (Wiedenbeck *et al.* 1995, Black *et al.* 2003, Elhlou *et al.* 2006). Prior to LA-ICP-MS analysis, CL and transmitted images were obtained from zircon crystals, so that the best sites for analysis could be chosen.

All analyses were performed using a Neptune multi-collector inductively plasma mass spectrometer (ICP–MS) coupled with an Analyte G2 excimer laser ablation (LA) system. The analyses were conducted in groups of 13 samples, each sample providing 40 sequential measurements (integration time ca. 1 s/cycle). Seven isotopes signals were synchronously measured: four in Faraday cups (greatest amplitude): 206, 208, 232, 238 and three in Multiple Ion Counters (greater sensitivity): 202, 204 and

**Table 1.** SHRIMP U, Th/U, percentage of Concordia discordance, dates ± 1 sigma error (Ma), isotopic ratios ± 1% error from the granitoids of Cordillera Real (Iriarte *et al.* 2021). Ranges from 298 to 479 Ma, n = 20 (in italic) were excluded for statistical comparison with the Ordovician units. Highly discordant zircon spots are discussed by Cordani *et al.* (2019). Errors in U/Pb ages are ± 1 sigma (corresponding to ~1% of calculated age).

| Pluton | Sample | U | Th/U | % Disc. | 207Pb/206Pb (Ma) | ±1s (Ma) | 206Pb/238U (Ma) | ±1s (Ma) | 207Pb*/235U | ±% | 206Pb*/238U | ±% | err corr |
|---|---|---|---|---|---|---|---|---|---|---|---|---|---|
| Huato n = 3 | RIB-27 | 135 | 0.131 | +5 | 314 | 427 | 299 | 5 | 0.350 | 18.8 | 0.048 | 1.70 | 0.1 |
| | RIB-27 | 477 | 0.591 | -0 | 609 | 24 | 610 | 7 | 0.823 | 1.6 | 0.099 | 1.20 | 0.8 |
| | RIB-27 | 235 | 0.095 | +0 | 793 | 23 | 790 | 9 | 1.180 | 1.6 | 0.130 | 1.20 | 0.7 |
| Illampu n = 6 | RIB-15 | 317 | 0.5 | +1 | 471 | 61 | 469 | 5 | 0.590 | 3 | 0.075 | 1.10 | 0.4 |
| | RIB-15 | 395 | 1.4 | +1 | 583 | 34 | 579 | 6 | 0.770 | 1.9 | 0.094 | 1.10 | 0.6 |
| | RIB-15 | 76 | 0.52 | +6 | 645 | 185 | 610 | 8 | 0.840 | 8.7 | 0.099 | 1.40 | 0.2 |
| | RIB-15 | 247 | 0.46 | -2 | 1,073 | 24 | 1,091 | 11 | 1.910 | 1.7 | 0.184 | 1.1 | 0.7 |
| | RIB-15 | 159 | 0.29 | +41 | 1,937 | 20 | 1,217 | 13 | 3.400 | 1.6 | 0.208 | 1.2 | 0.7 |
| | RIB-15 | 164 | 0.61 | +5 | 2,132 | 17 | 2,046 | 21 | 6.830 | 1.5 | 0.374 | 1.2 | 0.8 |
| Huayna Potosí n = 19 | RIB-2 | 931 | 0.16 | -4 | 300 | 46 | 312 | 6 | 0.358 | 2.7 | 0.050 | 1.8 | 0.7 |
| | RIB-20 | 533 | 0.2 | +74 | 1,600 | 29 | 454 | 8 | 0.993 | 2.4 | 0.0730 | 1.9 | 0.8 |
| | RIB-4 | 500 | 0.04 | +16 | 458 | 33 | 385 | 9 | 0.477 | 2.9 | 0.062 | 2.5 | 0.9 |
| | RIB-4 | 279 | 0.48 | +20 | 579 | 30 | 468 | 7 | 0.616 | 2 | 0.075 | 1.5 | 0.7 |
| | RIB-22 | 154 | 0.61 | +38 | 786 | 42 | 500 | 8 | 0.726 | 2.6 | 0.081 | 1.6 | 0.6 |
| | RIB-2 | 175 | 0.44 | +16 | 599 | 44 | 509 | 44 | 0.678 | 2.5 | 0.082 | 1.5 | 0.6 |
| | RIB-22 | 301 | 0.28 | +16 | 865 | 28 | 733 | 7 | 1.127 | 1.7 | 0.120 | 1.0 | 0.6 |
| | RIB-22 | 290 | 0.25 | +14 | 878 | 21 | 759 | 6 | 1.177 | 1.3 | 0.125 | 0.8 | 0.6 |
| | RIB-2 | 1,282 | 0.03 | -0 | 573 | 14 | 573 | 8 | 0.759 | 1.5 | 0.093 | 1.4 | 0.9 |
| | RIB-2 | 28,696 | 0.01 | -23 | 474 | 24 | 577 | 13 | 0.730 | 2.5 | 0.094 | 2.3 | 0.9 |
| | RIB-19 | 225 | 0.59 | +6 | 633 | 32 | 599 | 5 | 0.817 | 1.7 | 0.097 | 0.9 | 0.5 |
| | RIB-2 | 437 | 0.64 | +1 | 606 | 15 | 602 | 6 | 0.810 | 1.2 | 0.098 | 1.0 | 0.8 |
| | RIB-2 | 636 | 0.06 | +10 | 881 | 12 | 801 | 13 | 1.248 | 1.8 | 0.132 | 1.7 | 0.9 |
| | RIB-2 | 456 | 0.16 | +21 | 1,472 | 8 | 1,186 | 22 | 2.568 | 2.1 | 0.202 | 2.1 | 1.0 |
| | RIB-4 | 253 | 0.4 | +6 | 1,439 | 10 | 1,364 | 18 | 2.945 | 1.6 | 0.236 | 1.5 | 0.9 |
| | RIB-20 | 121 | 0.27 | +34 | 2,023 | 13 | 1,413 | 18 | 4.210 | 1.6 | 0.245 | 1.4 | 0.9 |
| | RIB-4 | 393 | 0.68 | +16 | 1,934 | 6 | 1,655 | 21 | 4.784 | 1.5 | 0.293 | 1.4 | 1.0 |
| | RIB-4 | 68 | 0.33 | +2 | 2,058 | 13 | 2,026 | 29 | 6.470 | 1.8 | 0.369 | 1.7 | 0.9 |
| | RIB-4 | 313 | 0.54 | +24 | 2,600 | 4 | 2,070 | 18 | 9.105 | 1.1 | 0.379 | 1.0 | 1.0 |
| | RIB-30 | 18,333 | 0.024 | -34 | 224 | 47 | 298 | 3 | 0.331 | 2.2 | 0.047 | 0.86 | 0.4 |
| | RIB-30 | 15,654 | 0.014 | -6 | 283 | 35 | 301 | 2 | 0.342 | 1.8 | 0.048 | 0.82 | 0.5 |
| | RIB-30 | 15,917 | 0.006 | -41 | 216 | 58 | 303 | 3 | 0.335 | 2.7 | 0.048 | 0.92 | 0.3 |
| | RIB-30 | 17,698 | 0.006 | -50 | 205 | 52 | 306 | 3 | 0.337 | 2.4 | 0.049 | 0.89 | 0.4 |
| | RIB-5 | 197 | 0.25 | +30 | 462 | 87 | 326 | 4 | 0.402 | 4.1 | 0.052 | 1.1 | 0.3 |
| | RIB-5 | 36,691 | 0.005 | -58 | 212 | 17 | 331 | 5 | 0.366 | 1.7 | 0.053 | 1.5 | 0.9 |
| | RIB-5 | 1,958 | 0.15 | +4 | 349 | 15 | 335 | 5 | 0.393 | 1.5 | 0.053 | 1.4 | 0.9 |
| | RIB-5 | 15,652 | 0.005 | -11 | 314 | 26 | 348 | 5 | 0.403 | 1.8 | 0.055 | 1.5 | 0.8 |
| | RIB-5 | 8,353 | 0.005 | -32 | 273 | 16 | 359 | 11 | 0.408 | 3.2 | 0.057 | 3.1 | 1.0 |
| | RIB-5 | 705 | 0.23 | +11 | 443 | 32 | 395 | 5 | 0.485 | 2.0 | 0.063 | 1.4 | 0.7 |
| | RIB-5 | 1,306 | 0.05 | +38 | 659 | 44 | 415 | 5 | 0.565 | 2.5 | 0.067 | 1.4 | 0.6 |
| | RIB-5 | 16,273 | 0.01 | -157 | 182 | 14 | 457 | 17 | 0.504 | 3.9 | 0.074 | 3.8 | 1.0 |
| | RIB-5 | 759 | 0.23 | +11 | 534 | 24 | 479 | 6 | 0.619 | 1.8 | 0.077 | 1.4 | 0.8 |
| | RIB-30 | 488 | 0.38 | +4 | 529 | 27 | 507 | 6 | 0.654 | 1.7 | 0.082 | 1.2 | 0.7 |
| | RIB-5 | 2,261 | 0.01 | -7 | 502 | 17 | 537 | 5 | 0.686 | 1.2 | 0.087 | 1.0 | 0.8 |
| | RIB-5 | 296 | 0.35 | -3 | 542 | 31 | 557 | 6 | 0.725 | 1.7 | 0.090 | 1.0 | 0.6 |
| | RIB-5 | 662 | 0.37 | -1 | 573 | 20 | 579 | 6 | 0.767 | 1.4 | 0.094 | 1.1 | 0.8 |

**Table 1.** Continuation.

| Pluton | Sample | U | Th/U | % Disc. | $^{207}Pb/^{206}Pb$ (Ma) | ±1s (Ma) | $^{206}Pb/^{238}U$ (Ma) | ±1s (Ma) | $^{207}Pb^*/^{235}U$ | ±% | $^{206}Pb^*/^{238}U$ | ±% | err corr |
|---|---|---|---|---|---|---|---|---|---|---|---|---|---|
| | RIB-5 | 312 | 0.19 | +55 | 1,286 | 27 | 607 | 9 | 1.139 | 2.1 | 0.099 | 1.6 | 0.8 |
| | RIB-5 | 421 | 0.3 | +48 | 1,579 | 71 | 869 | 32 | 1.942 | 5.5 | 0.144 | 4.0 | 0.7 |
| | RIB-30 | 201 | 0.228 | +18 | 1,167 | 34 | 974 | 13 | 1.771 | 2.2 | 0.163 | 1.4 | 0.6 |
| | RIB-5 | 792 | 0.05 | +50 | 1,840 | 7 | 987 | 9 | 2.566 | 1.1 | 0.165 | 1.0 | 0.9 |
| | RIB-5 | 227 | 0.6 | -4 | 986 | 18 | 1,020 | 10 | 1.701 | 1.4 | 0.171 | 1.1 | 0.8 |
| | RIB-5 | 161 | 0.34 | +0 | 1,149 | 24 | 1,148 | 12 | 2.099 | 1.6 | 0.195 | 1.1 | 0.7 |
| Zongo n = 30 | RIB-30 | 191 | 0.33 | +5 | 1,291 | 42 | 1,228 | 17 | 2.429 | 2.7 | 0.210 | 1.5 | 0.6 |
| | RIB-30 | 89 | 0.79 | -2 | 1,425 | 111 | 1,451 | 27 | 3.131 | 6.2 | 0.252 | 2.1 | 0.3 |
| | RIB-5 | 291 | 0.89 | +12 | 1,675 | 21 | 1,503 | 19 | 3.721 | 1.8 | 0.263 | 1.4 | 0.8 |
| | RIB-5 | 151 | 0.62 | +2 | 1,661 | 12 | 1,638 | 16 | 4.070 | 1.3 | 0.289 | 1.1 | 0.9 |
| | RIB-30 | 119 | 0.4 | +19 | 1,993 | 14 | 1,661 | 25 | 4.966 | 1.9 | 0.294 | 1.7 | 0.9 |
| | RIB-5 | 106 | 0.53 | -1 | 1,802 | 22 | 1,824 | 24 | 4.965 | 2.0 | 0.327 | 1.5 | 0.8 |
| | RIB-30 | 16,246 | 0.004 | +13 | 2,603 | 10 | 2,323 | 33 | 10.451 | 1.8 | 0.434 | 1.7 | 0.9 |
| Taquesi n = 2 | RIB-11 | 226 | 0.6 | +2 | 582 | 34 | 573 | 15 | 0.761 | 3.1 | 0.093 | 2.7 | 0.9 |
| | RIB-12 | 211 | 0.6 | +25 | 698 | 44 | 530 | 8 | 0.740 | 2.6 | 0.086 | 1.61 | 0.6 |
| | *RIB-43* | *740* | *0.2* | *+66* | *907* | *29* | *324* | *3* | *0.492* | *1.7* | *0.052* | *0.9* | *0.5* |
| Quimsa Cruz n = 4 | RIB-43 | 257 | 0.4 | +1 | 606 | 33 | 600 | 5 | 0.807 | 1.8 | 0.097 | 0.9 | 0.5 |
| | RIB-46 | 367 | 0.6 | +7 | 1,707 | 7 | 1,608 | 12 | 4.087 | 0.9 | 0.283 | 0.82 | 0.9 |
| | RIB-46 | 121 | 0.8 | -0 | 1,645 | 30 | 1,648 | 28 | 4.063 | 2.5 | 0.291 | 1.93 | 0.8 |

207. The U–Pb analysis was done in the following order: two blanks, two NIST standard glasses, three external standards, 13 unknown samples, two external standards, and two blanks. An interpolation of the four blank measurement sequences, two before and two after the samples (bracketing method), was subtracted from each one of the seven measured masses (202, 204, 206, 207, 208, 232 and 238).

A final bracketing (three before and two after the samples) of the standard minerals was then used to correct the effect of the fractionation on the four ratios ($^{206}Pb/^{238}U$, $^{207}Pb/^{235}U$, $^{207}Pb/^{206}Pb$, $^{208}Pb/^{232}Th$), before they could finally be extrapolated through best line fits to t = 0 and then used to calculate the respective ages. Errors in all simple arithmetic operations were algebraically propagated. Least-squares fitting was the choice for the best line fits and, on all final results and plots, the $2\sigma$ error calculated by Isoplot 3.70 (Ludwig 2009) was adopted. CL images are shown in Figures 2 and 3. Analytical data are shown in the Supplementary Table 1.

## HISTOGRAM AND STATISTICAL ANALYSES

Figure 4 is a probability density plot of the $^{206}Pb/^{238}U$ xenocrystic zircon ages of the CRGs, and Figures 3 and 4 are probability density plots of $^{206}Pb/^{238}U$ detrital zircon ages for samples RIB-51 (sandstone of the Amutara Formation) and RIB-57 (schist from the Coroico Formation). To build the histograms we used $^{206}Pb/^{238}U$ values for ages up to 1300 Ma and $^{207}Pb/^{206}Pb$ values for ages older than 1300 Ma. We chose values with a concordance range of 100 ± 10% only. The histograms were built using the Isoplot software (Ludwig 2009) and their "x" axes were set to match those by Chew *et al.*

(2008) in their study of detrital zircon provenance of the Central Andes.

The histogram of the CRGs (Fig. 4) shows the highest peak ranging from 490 to 640, characterized by several smaller peaks within that interval. Smaller peaks of older ages are widespread between 700 to 2300 Ma. Observed intervals are at 700–900, 950–1050, 1100–1300, 1300–1500, 1600–1700, 1750–1850, 2000–2100 and 2300 Ma.

For RIB-51 sandstone (Fig. 5), the highest peak is within the range of 500 to 750 Ma. The weighted mean age of younger grains (n = 10) was 533 ± 7 Ma. The overall spread of ages is from 800 to 2900 Ma. Observed intervals are at 800–900, 1000–1100, 1100–1350 and 1350–1600. Individual grains are at 1750, 1950, 2350, 2650, 2750 and 2900 Ma.

For RIB-57 schist (Fig. 6), the highest peak is within the range of 480 to 700 Ma. The weighted mean age of younger grains (n = 8) was 527 ± 8 Ma. Smaller peaks at 750–800, 900, 1150, 1350, 1400, 1700–1800, and 1850–2150 Ma.

In order to have a better picture of the detrital material deposited on the Ordovician western margin of Gondwana, the probability density plots of the Bolivian samples RIB-51 and RIB-57 were compared with similar diagrams for Ordovician sedimentary rocks in south-eastern Peru. These data were taken from Reimann *et al.* (2010), whose work included samples San-12 and San-17 from the Sandia Formation, which consists of 1,500 to 2,000 m thick sequences of sandstone and siltstone. In the same article, two other samples, Cor-18 and Am-20, from the Amutara Formation in Bolivia, were also considered for comparison.

Figure 7 shows the whole set of stacked histograms and Figure 8 shows the location of all these samples, with their respective histogram. The probability density plot of the
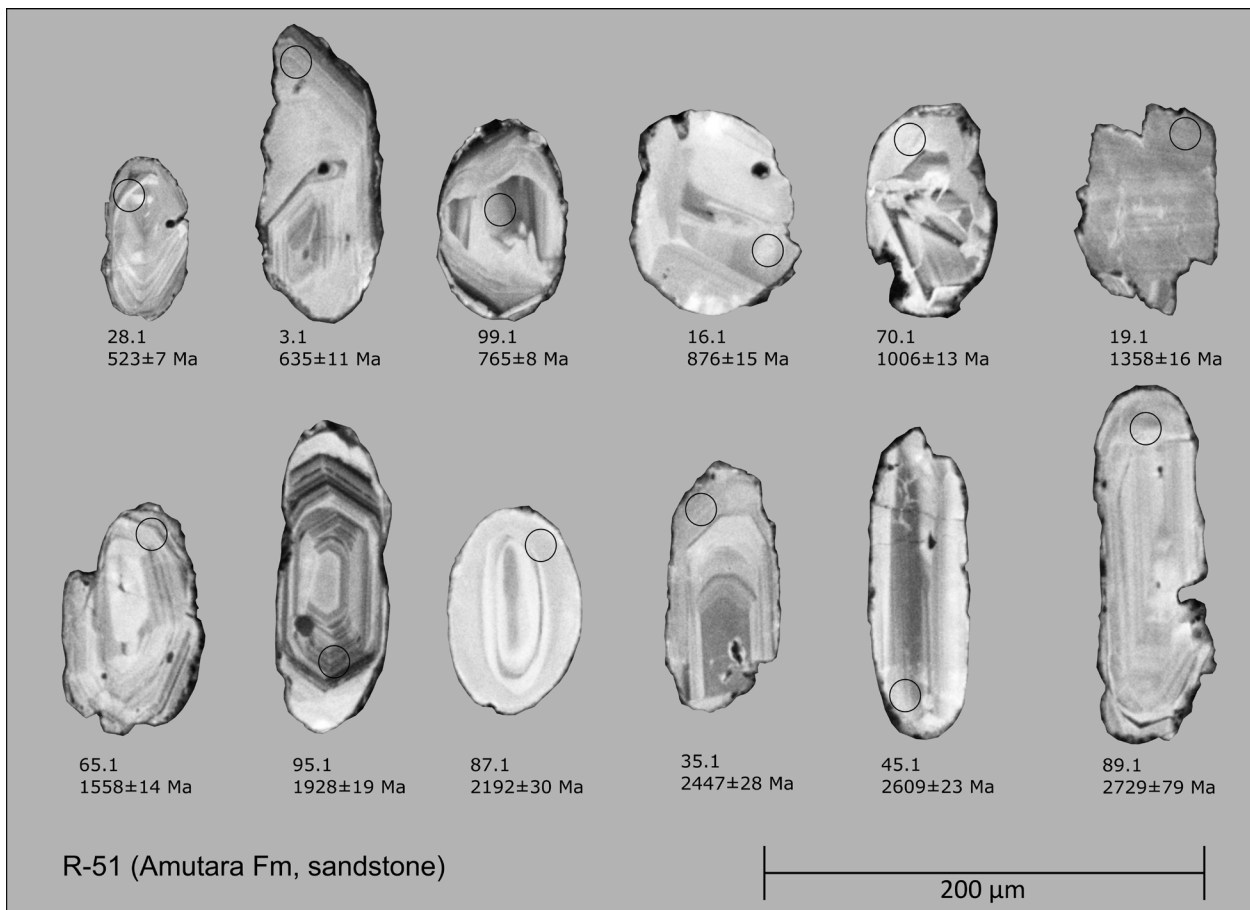
**Figure 2.** CL images of selected detrital zircons for sample RIB-51 (sandstone, Amutara Fm.). Spot site is marked by a circle.
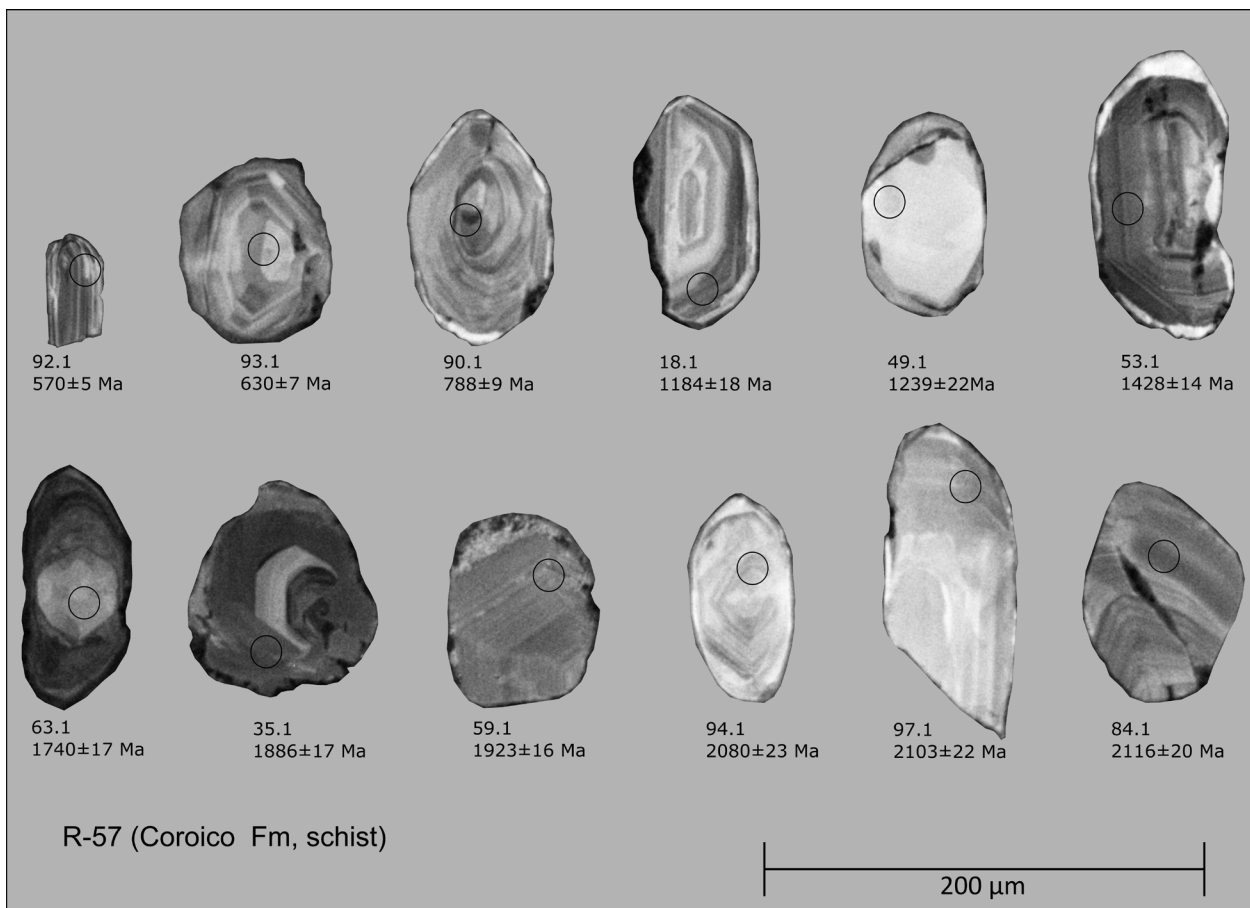


**Figure 3.** CL images of selected detrital zircons for sample RIB-57 (schist, Coroico Fm.). Spot site is marked by a circle.
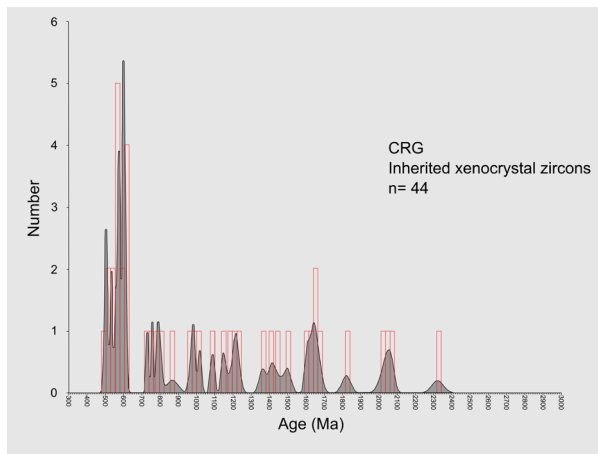
**Figure 4.** Probability density plot of the $^{206}Pb/^{238}U$ xenocrystic zircon ages for Cordillera Real granitoids (CRGs).
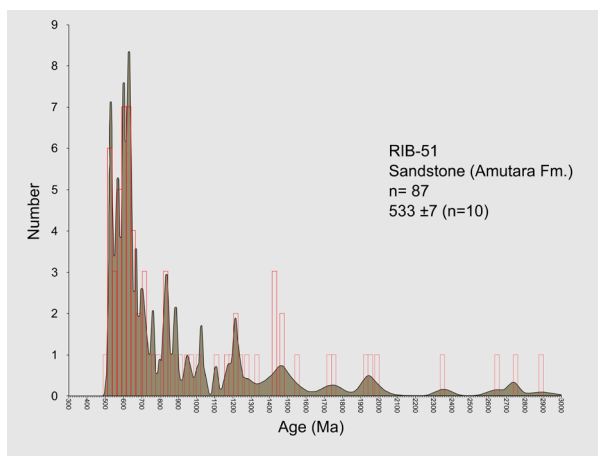


**Figure 5.** Probability density plot of the $^{206}Pb/^{238}U$ detrital zircon ages for sample RIB-51, corresponding to a sandstone from the Ordovician Amutara Fm. The age shown corresponds to the youngest population-weighted mean.
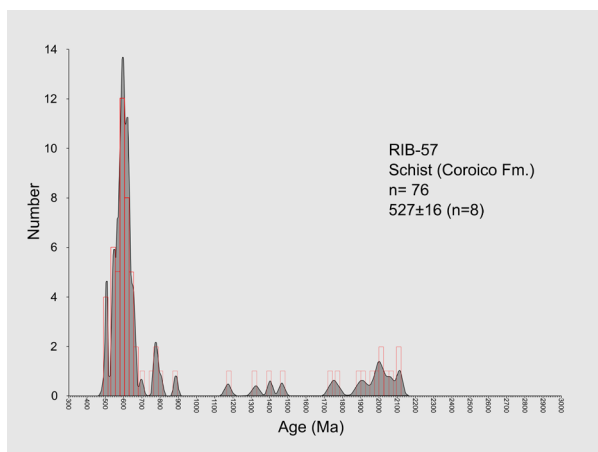


**Figure 6.** Probability density plot of the $^{206}Pb/^{238}U$ detrital zircon ages for sample RIB-57, corresponding to schist from the Ordovician Coroico Fm. The age shown corresponds to the youngest population-weighted mean.

xenocrystal zircons of the granitic plutons is also included in the figure. It is remarkable how the six Ordovician samples, as well as the xenocrystal zircons, show a very similar pattern,

with notable peaks at 750–530 Ma, related to Neoproterozoic to Cambrian sources.

The Kolmogorov-Smirnov test (K-S) was employed to investigate the distribution and affinity of ages between the inherited zircon age population of the CRG, and the detrital zircon age population of the Ordovician units. The p-values of the K-S test (Conover 1971) are used to calculate the probability of a pair of samples being from the same source. We reject the hypothesis that two samples came from the same source when the probability is lower than 0.05. Higher values indicate nearly identical age spectra (Berry *et al.* 2001).

Table 2 shows the calculated p-values and the density curves of the histograms of Figures 7 and 8, calculated using "R" software (R Core Team 2020). The samples seem to be quite related to each other, except for RIB-57, whose p-value does not show any relationship with the other datasets. Maybe this could be related to some difference in its age of deposition. Similarly, sample Am-20 is highly related to San-12, but shows less correlation with the others.

## DISCUSSION

In order to better understand and compare the U/Pb ages of detrital zircons from sedimentary country rocks with those of xenocrystal inheritance of CRGs, and to picture the potential paleo-relief in South America during Triassic times, we will analyze the age distribution of Figures 7 and 8.

In Figures 7 and 8, we compile U/Pb detrital zircon age from the database of Reimann *et al.* (2010) along with our two samples, RIB-51 and RIB-57, and the inherited xenocrystal zircon ages of CRGs (Iriarte *et al.* 2021). All the sedimentary formations are from the upper Ordovician. We will discuss the most noticeable peaks seen on the histograms of Figure 7 and correlate them to major known geological events of the region.

Histograms in Figure 8 include the CRG xenocrysts. They share a common feature of noticeable peaks at 500 to 750 Ma along with different distribution of older ages. It was shown that they could be related to a common source. Ordovician ages corresponding to the Famatinian arc (upper Cambrian to early Ordovician, Otamendi *et al.* 2012) are scarce. There are also smaller peaks of Grenvillian ages (~1000 Ma). These Grenvillian peaks are frequent along the Central Andes (Bahlburg *et al.* 2011, Rezende de Oliveira *et al.*, 2017; Ramos 2010, 2018). Finally, there is an older population from 1650 to 2700 Ma. We will discuss the possible sources of these detrital grains.

Because of its proximity, it is expected that the source of these detrital zircon lies in the Amazonian craton that exposes extensive Paleo to Mesoproterozoic rocks covering older Archean cores. Single zircon ages from 1650 to 2700 Ma can be the result of these older units being recycled from the Amazonian craton (e.g., RNJ to CA provinces of Fig. 9).

The Neoproterozoic to Cambrian ages (500 to 1000 Ma) show larger peaks from 500 to 600 Ma (Cambrian to Ediacaran) along with smaller peaks from 600 to 700 Ma (Cryogenian) and from 700 to 1000 Ma (Tonian). These probably reflect the recycling of magmatic and metamorphic rocks. Belts uplifted during 500 to 900 Ma along the Trans Brazilian-Kandi lineament
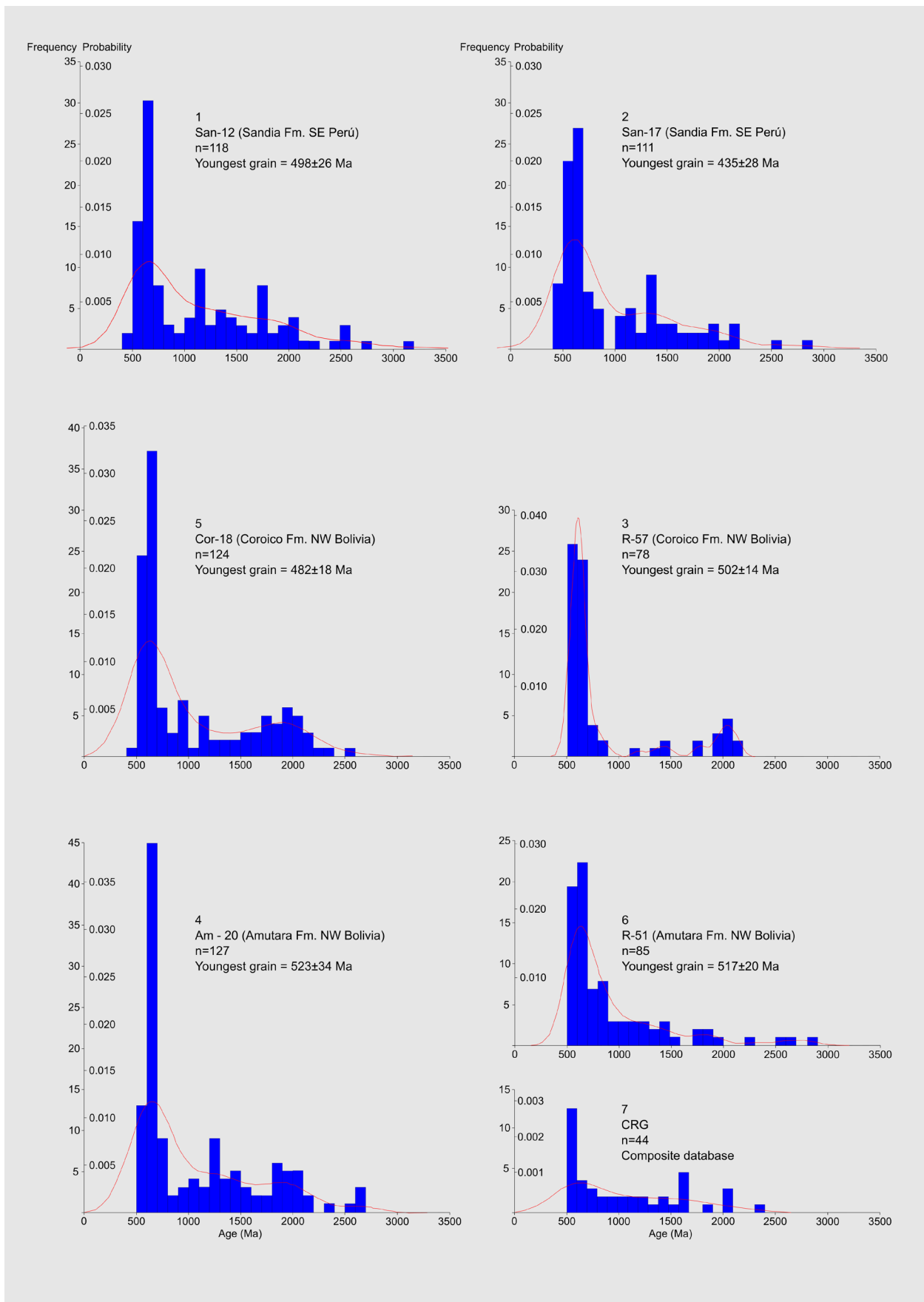
**Figure 7.** Stacked histograms showing U/Pb zircon age distribution for samples of the Sandia, Amutara, and Coroico formations, as well as CRG inherited xenocrysts. Data sources are from Reimann *et al.* (2010) and Iriarte *et al.* (2021).

(Cordani *et al.* 2020) and/or the Pampean belts (Escayola *et al.* 2011) could be the primary source of detrital zircons (Fig. 8). Other candidates could be the "hidden Neoproterozoic belt"

within the Andes itself (Chew *et al.* 2008, Bahlburg *et al.* 2011) or recycling of previous sedimentary rocks (e.g. Tucavaca basin, McNamee 2001).
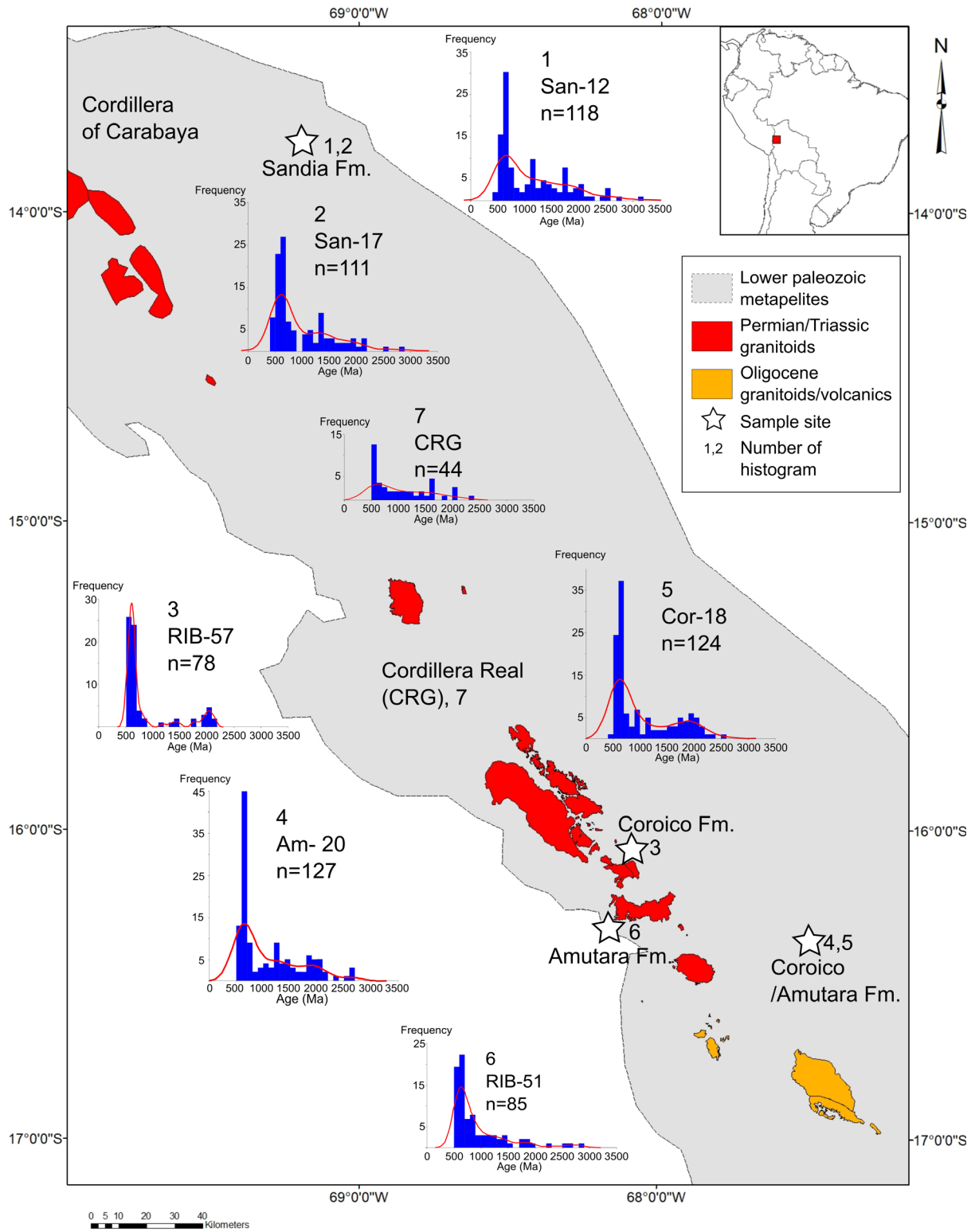
**Figure 8.** Granitoids and their early Paleozoic country rocks along with histograms showing zircon age distribution. Outcrops of Lower Paleozoic sedimentary units were taken and modified from Cordani *et al.* (2016).

**Table 2.** Calculated p-values using the K-S test (pairs with p-values < 0.05 are not correlated).

| | San-12 | San-17 | Cor-18 | Am-20 | RIB-51 | RIB-57 | CRG |
|---|---|---|---|---|---|---|---|
| San-12 | | 0.245 | 0.179 | 0.615 | 0.017 | 0.000 | 0.340 |
| San17 | | | 0.108 | 0.019 | 0.584 | 0.007 | 0.407 |
| Cor-18 | | | | 0.031 | 0.216 | 0.011 | 0.425 |
| Am-20 | | | | | 0.091 | 0.000 | 0.238 |
| RIB-51 | | | | | | 0.012 | 0.128 |
| RIB-57 | | | | | | | 0.004 |
| CRG | | | | | | | |
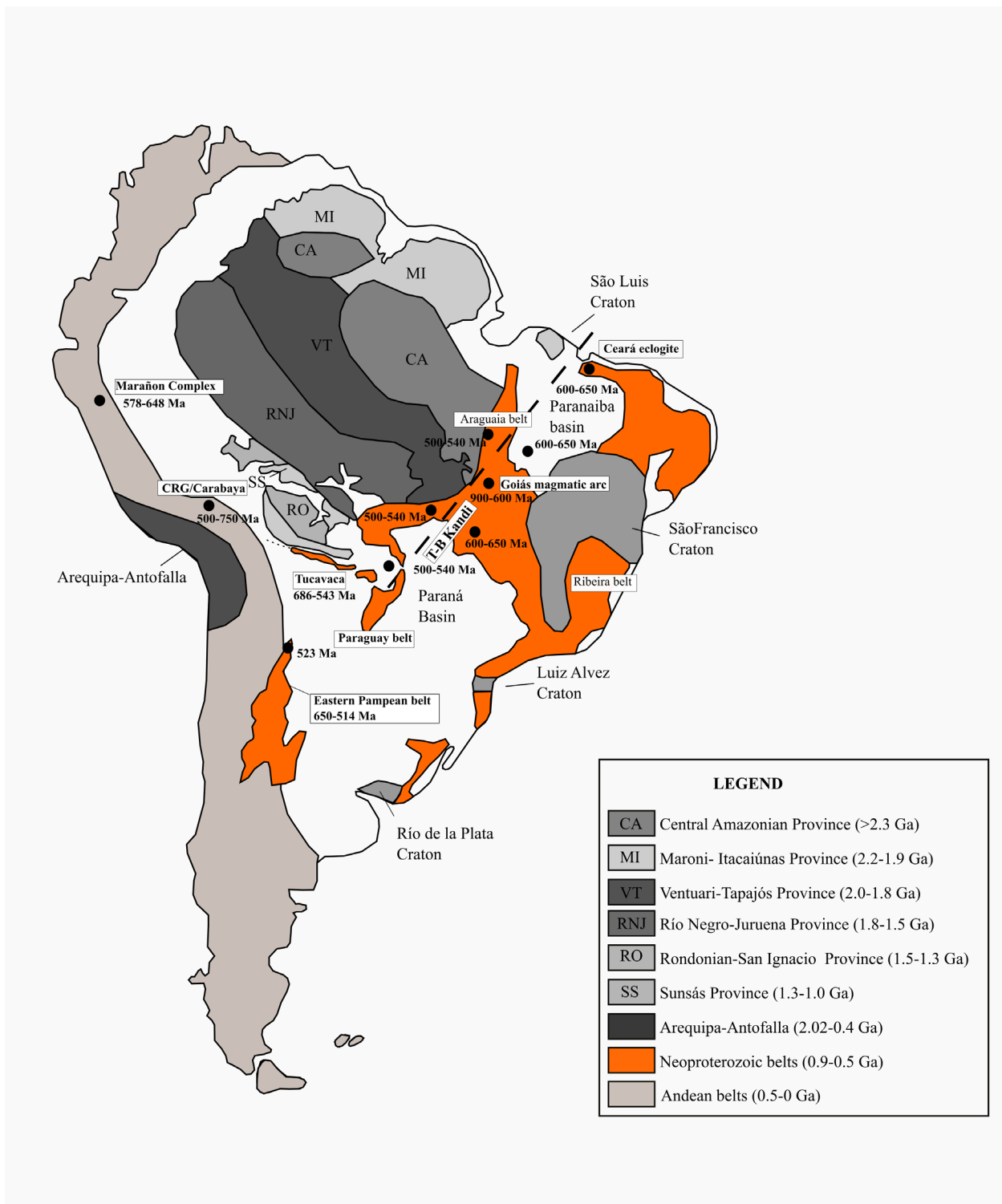
Source: modified from Cordani *et al.* (2020) and Collo *et al.* (2009).
**Figure 9.** Distribution of Neoproterozoic belts on the South American continent along with main geological provinces. Neoproterozoic ages were compiled from Moura *et al.* (2008), Manzano *et al.* (2008), Escayola *et al.* (2007), and Pimentel (2016).

## Source 1: Transbrazilian-Kandi Lineament

Reimann *et al.* (2010) inferred Brasiliano sources (450–700 Ma) probably to the east. In this sense, important relief was produced during the Brasiliano orogenic cycle, with the closure of the Goiás-Pharusian Ocean, along the Trans-Brazilian-Kandi lineament, a place where successive sutures and collisions occurred (Fig. 9, Cordani *et al.* 2020). By that time, Gondwana had become almost completely assembled. In the transition from Rodinia to Gondwana,

the Goiás-Pharusian Ocean was consumed by means of subduction-to-collision, roughly between 900 and 500 Ma. This process formed juvenile arcs and a large volume of granitoids (Goiás and Santa Quitéria, Ganade de Araujo *et al.* 2014). This was followed by a continental collision between Amazonia and Congo, forming a Himalayan type relief (700-540 Ma, Cordani *et al.* 2020).

This Goiás magmatic arc is a major area of collision and accretion of the Amazonian Craton margin made up essentially

by Neoproterozoic granitoids with juvenile signatures and predominantly calc-alkaline chemistry related to subduction (Ganade de Araujo *et al.* 2014, Pimentel 2016). U-SHRIMP ages on overgrowth rims of zircon of eclogites in NE Brazil (Ceará) yielded ca. 616. Granitoids and gneisses, which supply detrital zircons, are formed under this high to moderate regional metamorphism, at 15-25 km deep. They are exhumed during the rise of mountain belts. When eclogites that form at depths greater than 100 km are exhumed, the result is a Himalayan type cordillera (10 km high).

These high Himalayan-like mountains could have persisted at least until 540 Ma as estimated from the age of several post-collisional granitoids (Ganade de Araujo *et al.* 2014). The oldest orogenic belt of this "modern type plate tectonics" is, in fact, associated with the formation of Western Gondwana.

This could be the main source of detrital zircon of 900 to 600 Ma, with a predominance of Ediacaran ages (650-600 Ma). Terrains of these ages may lie beneath the sediments of the Paraná, Paranaiba, and Pampean basins (Fig. 9). To the west of the TB-Kandi lineament, the Ediacaran sedimentary sequence of the Paraguay belt bears detrital zircons of that interval of age (Chamani *et al.* 2011).

In other regions, this Neoproterozoic age peak is absent. For instance, in the Araguaia aulacogen, detrital zircons do not bear Brasiliano ages (Pinheiro *et al.* 2003, Barros and Gorayeb *et al.* 2019) showing instead, a major peak of Grenvillian age (1000 Ma). Cambrian ages of granites in the Paraguay belt and post-tectonic granites in the Brasiliano belts could also mean potential sources, although they represent a smaller area.

## Source 2: Pampean Belt

An important relief was also associated with the closure of the Puncoviscana Ocean during the Cambrian Pampean orogeny (Larrovere *et al.* 2021), which occurred throughout larger parts of the Sierras Pampeanas. This relief was created by a collision between the Arequipa-Antofalla block and the western part of Pampia (Escayola *et al.* 2011). Today, the whole area is covered by modern sediment. This Cambrian relief, exposing peraluminous granitoids, could be also the source of detrital zircon deposited in the Ordovician basins.

## Source 3: Central Andes

Chew *et al.* (2008) suggested the presence of Neoproterozoic orogenic belts within the Central Andes that are covered by younger sediments. The study of Bahlburg *et al.* (2011) on Hf isotopes in zircon also suggested the presence of Neoproterozoic magmatic belts within the Central Andes. Their study shows the presence of juvenile and evolved Neoproterozoic zircon, suggesting the reworking of juvenile and evolved magmatic or metamorphic rocks. This "hidden" belt could be the continuation of the Pampean belts towards the Marañon complex of northern Peru (Chew *et al.* 2008, Cardona *et al.* 2009).

## Source 4: recycling of pre-existing sedimentary sources — Tucavaca Basin

Primary Cambrian to Neoproterozoic sources could be eroded, transported, and deposited in several sub-basins (e.g., Tucavaca) and then recycled and re-deposited in the Ordovician units.

The closest Neoproterozoic outcrop to the Cordillera Real is located in the Tucavaca basin, near the SE border of Bolivia, next to the Amazonian shield (Durand 1993, McNamee 2001, Ramos 2008). It is part of the Paraguay belt and is characterized by clastic and carbonate sedimentary sequences deposited along a rifted basin (500 x 60 km), striking N 40° W. Ramos (2008), interpreted it as an "aulacogen" pointing towards the Andes.

Basement units on the Paraguayan side were dated by Mcgee *et al.* (2015) using LA-ICP-MS technique and yielded a U/Pb age of 686 ± 2 Ma. For the upper part, the Corumbá Group in Brazil (equivalent to the carbonate Murciélago Formation in Bolivia), a U/Pb age of 543 ±2 Ma was obtained (Souza de Alvarenga *et al.* 2011). Thus, the deposition of Tucavaca basin can be constrained between 686 and 543 Ma (Fig. 8).

Detrital zircons in the Paraguay belt basins are mainly Ediacaran (Babinski *et al.* 2013, McGee *et al.* 2015, Vasconcelos 2018), so the sediments of the Tucavaca basin may bear detrital zircon grains of that age as well. Their original source could be located within the Brasiliano or Pampean belts. It is possible that, subsequently, the "Tucavaca Trough" acted as a positive relief whose rocks were eroded and deposited in the Ordovician basins. It is also possible that Neoproterozoic rocks were recycled more than once over time. Other possible sources of recycled Neoproterozoic zircon ages could be the Cambrian Sama Fm. of southern Bolivia and the clastic to carbonate sequences of the Limbo Group in the core of the Eastern Cordillera (Suárez-Soruco 2000).

## CONCLUSIONS

The age distribution of both sedimentary sequences and the xenocrysts of CRGs, as well as their statistical relationship and geochemical evidence support processes such as AFC as plausible during emplacement.

Based on this geochronological record, we can suggest potential sources of these detrital zircons, as well as a better picture of the potential paleo-relief in South America during Ordovician to Triassic times.

Ordovician sedimentary sequences from SE Peru and NW Bolivia received zircon grains from the same sources. The main source is Neoproterozoic to Cambrian in age and probably is derived from mountains formed during the Brasliano cycle through the Tranbrazilian-Khandi tectonic corridor. We cannot rule out sources related to the Sierras Pampeanas, Neoproterozoic belts hidden within the Central Andes, or recycled from pre-existent sedimentary units (such as the Tucavaca basin). Older sources (> 1000 Ma) possibly lie within the Amazonian craton. Finally, the Triassic plutons of the Cordilleras Real and Carabaya incorporated a large amount of Famatinian to Gondwanian detrital zircons, taken from their host basement or recycled from the Andean Paleozoic, mainly the Amutara Fm., or equivalents (such as the Sandia Fm.).

## ACKNOWLEDGMENTS

### ARTICLE INFORMATION

## REFERENCES

Ávila W.A. 1990. Tin-bearing granites from the Cordillera Real, Bolivia; A petrological and geochemical review. *In*: Kay S.M., Rapela C.W. (Eds.). *Plutonism from Antarctica to Alaska*. America, Geological Society of America, Special paper, 241, p. 145-159.

Babinski M., Boggiani P.C., Trindade R.I.F., Fanning C.M. 2013. Detrital zircon ages and geochronological constraints on the Neoproterozoic Puga diamictite and associated BIFs in the southern Paraguay Belt, Brazil. *Gondwana*, **23**(3):988-997. http://dx.doi.org/10.1016/j.gr.2012.06.011

Bahlburg H., Vervoort J.D., DuFrane A.S., Carlotto V., Reimann C., Cárdenas J. 2011. The U-Pb and Hf isotope evidence of detrital zircons of the Ordovician Ollantaytambo Formation, southern Peru, and the Ordovician provenance and paleogeography of southern Peru and northern Bolivia. *Journal of South American Earth Sciences*, **32**(3):196-209. https://doi.org/10.1016/j.jsames.2011.07.002

Barros L.D., Gorayeb P.S.S. 2019. Serra do Tapa Ophiolite Suite - Araguaia Belt: Geological characterization and Neoproterozoic evolution (central-northern Brazil). *Journal of South American Earth Sciences*, **96**:102323. https://doi.org/10.1016/j.jsames.2019.102323

Black L.P., Kamo S.L., Allen C.M., Aleinikoff J.N., Davis D.W., Korsch R.J., Foudoulis C. 2003. Temora 1: A new zircon standard for Phanerozoic U-Pb geochronology. *Chemical Geology*, **200**(1-2):155-170. https://doi.org/10.1016/S0009-2541(03)00165-7

Berry R.F., Jenner G.A., Meffre S., Tubrett M.N. 2001. A North American provenance for Neoproterozoic to Cambrian sandstones in Tasmania? *Earth and Planetary Science Letters*, **192**(2):207-222. https://doi.org/10.1016/S0012-821X(01)00436-8

Calle A., Horton B.K., Garcia-Duarte R., Flaig P.P. 2017. Neoproterozoic-paleozoic tectonics and paleography of the West-Central South America convergent margin from detrital zircon geochronology. *In*: GSA Annual Meeting, Seattle, 2017. *Conference Paper*. The Geological Society of America. https://doi.org/10.1130/abs/2017AM-305408

Cardona A., Cordani U.G., Ruiz J., Valencia V.A., Armstrong R., Chew D., Nutman A., Sanchez A.W. 2009. U-Pb zircon geochronology and Nd isotopic signatures of the pre-mesozoic metamorphic basement of the eastern peruvian andes: Growth and provenance of a late neoproterozoic to carboniferous accretionary orogen on the northwest margin of gondwana. *Journal of Geology*, **117**(3):285-305. https://doi.org/10.1086/597472

Chamani M.A.C. 2011. *Tectônica intraplaca e deformacao sinsedimentar induzida por abalos sismicos: o Lineamento Transbrasiliano e estructiras relacionadas na Provincia Parnañiba, Brasil*. Tese de Doutorado, Universidade de São Paulo, São Paulo, SP, Brazil.

Chew D.M., Magna T., Kirkland C.L., Mišković A., Cardona A., Spikings R., Schaltegger U. 2008. Detrital zircon fingerprint of the Proto-Andes: Evidence for a Neoproterozoic active margin? *Precambrian Research*, **167**(1-2):186-200. https://doi.org/10.1016/j.precamres.2008.08.002

Collo G., Astini R.A., Cawood P.A., Buchan C., Pimentel M. 2009. U – Pb detrital zircon ages and Sm – Nd isotopic features in low-grade metasedimentary rocks of the Famatina belt: implications for late Neoproterozoic – early Palaeozoic evolution of the proto-Andean margin of Gondwana. *Journal of the Geological Society*, **166**(2):303-319. https://doi.org/10.1144/0016-76492008-051.U

Conover W.C. 1971. *Practical nonparametric statistics*. New York: John Wiley & Sons.

Cordani U.G., Fairchild T.R., Ganade C.E., Babinski M., Moraes Leme J. 2020. Dawn of metazoans: To what extent was this influenced by the onset of "modern-type plate tectonics"? *Brazilian Journal of Geology*, **50**(2):e20190095. https://doi.org/10.1590/2317-4889202020190095

Cordani U.G., Iriarte A.R., Sato K. 2019. Geochronological systematics of the Huayna Potosí, Zongo and Taquesi plutons, Cordillera Real of Bolivia, by the K/Ar, Rb/Sr and U/Pb methods. *Brazilian Journal of Geology*, **49**(2):e20190016. https://doi.org/10.1590/2317-4889201920190016

Cordani U.G., Ramos V.A., Fraga L.M., Cegarra M., Deldgado I., Souza K.G., Gomes F.E.M., Schobbenhaus C. 2016. *Tectonic Map of South America*. 2ª ed. Commission for the Geological Map of the World.

DePaolo D.J. 1981. Assimilation and isotopic effects of combined wallrock assimilation and fractional crystallization. *Earth and Planetary Science Letters*, **53**(2):189-202. https://doi.org/10.1016/0012-821X(81)90153-9

Durand FR. 1993. Las icnofacies del basamento metasedimentario en el Noroeste Argentino: Significado cronológico y aspectos paleogeográficos. In: XII Congr. Geol. Argent. *Actas…* 2:260-267.

Elhlou S., Belousova E., Griffin W.L., Pearson N.J., O'Reilly S.Y. 2006. Trace element and isotopic composition of GJ-red zircon standard by laser ablation. *Geochimica et Cosmochimica Acta*, **70**(18 Suppl.):A158. https://doi.org/10.1016/j.gca.2006.06.1383

Escayola M.P., Pimentel M.N., Armstrong R. 2007. Neoproterozoic backarc basin: Sensitive high-resolution ion microprobe UPb and Sm-Nd isotopic evidence from the Eastern Pampean Ranges, Argentina. *Geology*, **35**(6):495-498. https://doi.org/10.1130/G23549A.1

Escayola M.P., van Staal C.R., Davis W.J. 2011. The age and tectonic setting of the Puncoviscana Formation in northwestern Argentina: An accretionary complex related to Early Cambrian closure of the Puncoviscana Ocean and accretion of the Arequipa-Antofalla block. *Journal of South American Earth Sciences*, **32**(4):438-459. https://doi.org/10.1016/j.jsames.2011.04.013

Franz G., Lucassen F., Kramer W., Trumbull R.B., Trumbull Romer R.L., Wilke H.G., Viramonte J.G., Becchio R., Siebel W. 2006. Crustal evolution at the Central Andean continental margin: a geochemical record of crustal growth, recycling and destruction. *In*: Oncken O., Chong G., Franz G., Giese P., Gotze H.J., Ramos V.A., Strecker M., Wigger P. (eds.). *Frontiers in Earth Science*. The Andes Active Subduction Orogeny, p. 45-64. Cham: Springer.

Ganade de Araujo C.E., Rubatto D., Hermann J., Cordani U.G., Caby R., Basei M.A.S. 2014. Ediacaran 2,500-km-long synchronous deep continental subduction in the West Gondwana Orogen. *Nature Communications*, **5**:5198. https://doi.org/10.1038/ncomms6198

Gillis R.J., Horton B.K., Grove M. 2006. Thermochronology, geochronology, and upper crustal structure of the Cordillera Real: Implications for Cenozoic exhumation of the central Andean plateau. *Tectonics*, **25**(6):1-22. https://doi.org/10.1029/2005TC001887

Iriarte A.R., Cordani U.G., Sato K. 2021. Geochronology of the Cordillera Real granitoids, the inner magmatic arc of Bolivia. *Andean Geology*, 48(3):403-441. http://dx.doi.org/10.5027/andgeoV48n3-3326

Jiménez N., López-Velásquez S. 2008. Magmatism in the Huarina belt, Bolivia, and its geotectonic implications. *Tectonophysics*, **459**(1-4):85-106. https://doi.org/10.1016/j.tecto.2007.10.012

Keay S., Steele D., Compston W. 1999. Identifying granite sources by SHRIMP U-Pb zircon geochronology: An application to the Lachlan foldbelt. *Contributions to Mineralogy and Petrology*, **137**(4):323-341. https://doi.org/10.1007/s004100050553

Kontak D.J., Clark A.H., Farrar E., Archibald D.A., Baadsgaard H. 1990. Late Paleozoic-early Mesozoic magmatism in the Cordillera de Carabaya, Puno, southeastern Peru: Geochronology and petrochemistry. *Journal of South American Earth Sciences*, **3**(4):213-230. https://doi.org/10.1016/0895-9811(90)90004-K

Larrovere M.A., Casquet C.R., Aciar H.R., Baldo E.G., Alasino P.H., Rapela C.W. 2021. Extending the Pampean orogen in western Argentina: New evidence of Cambrian magmatism and metamorphism within the Ordovician Famatinian belt revealed by new SHRIMP U–Pb ages. *Journal of South American Earth Sciences*, **109**:103222. https://doi.org/10.1016/j.jsames.2021.103222

Ludwig K. 2009. *SQUID 2:* A User's Manual. Berkeley: Berkeley Geochronology Center, Special Publication, 5, 110 p.

Manzano J.C., Godoy A.M., Marques L., Araújo Marques Barbosa L. 2008. Contexto tectônico dos granitoides neoproterozoicos da faixa de dobramentos Paraguai, MS e MT. *Geociências*, **27**(4):493-507.

McGee B., Collins A.S., Trindade R.I.F., Payne J., 2015. Age and provenance of the Cryogenian to Cambrian passive margin to foreland basin sequence of the northern Paraguay Belt, Brazil. *GSA Bulletin*, **127**(1-2):76-86. https://doi.org/10.1130/B30842.1

McNamee J. 2001. The Tucavaca Through: Potential for Sedex type base metal/Ag mineralization in a late Proterozoic rift in Eastern Bolivia. Estilos de mineralización en Bolivia. *Colegio de Geologos de Bolivia*, 21-24.

Moura C.A.V., Pinheiro B.L.S., Nogueira A.C.R., Gorayeb P.S.S., Galarza M.A. 2008. Sedimentary provenance and palaeoenvironment of the Baixo Araguaia supergroup: Constraints on the palaeogeographical evolution of the Araguaia Belt and assembly of West Gondwana. *In*: Pankhurst R.J., Trouw R.A., Brito Neves B.B., De Wit M.J. (eds.). *West Gondwana:* Pre-Cenozoic Correlations Across the South Atlantic Region. The Geological Society of London. Special Publications, **294**(1):173-196. https://doi.org/10.1144/SP294.10

Otamendi J.E., Ducea M.N., Bergantz G.W. (2012). Geological, petrological and geochemical evidence for progressive construction of an Arc crustal section, sierra de valle fértil, famatinian Arc, Argentina. Journal of Petrology, **53**(4), 761-800. https://doi.org/10.1093/petrology/egr079

Pimentel M. 2016. The tectonic evolution of the Neoproterozoic Brasília Belt, central Brazil: a geochronological and isotopic approach. *Brazilian Journal of Geology*, **46**(Suppl. 1):67-82. https://doi.org/10.1590/2317-4889201620150004

Pinheiro B.L.S., Moura C.A.V., Klein E.L. 2003. Estudo de proveniência em arenitos das formações Igarapé de Areia e Viseu, nordeste do Pará, com base em datação de monocristais de zircão por evaporação de chumbo.

*In*: 8º Simpósio de Geologia da Amazônia, Manaus. *Resumos expandidos...* CD-ROM.

Ramos V.A. 2008. The basement of the Central Andes: the Arequipa and related terranes. *Annual Review of Earth and Planetary Sciences*, **36**(1):289-324. https://doi.org/10.1146/annurev.earth.36.031207.124304

Ramos V.A. 2010. The Grenville-age basement of the Andes. *Journal of South American Earth Sciences*, **29**(1):77-91. https://doi.org/10.1016/j.jsames.2009.09.004

Ramos V.A. 2018. Tectonic Evolution of the Central Andes: From Terrane Accretion to Crustal Delamination. In: Zamora G., McClay K.M., Ramos V.A. (eds.). Petroleum basins and hydrocarbon potential of the Andes of Peru and Bolivia. *AAPG Memoir*, 117, p. 1-34. https://doi.org/10.1306/13622115M1172855

R Core Team. 2020. *R:* A language and environment for statistical computing. Vienna, Austria: R Foundation for Statistical Computing. Available at: https://www.R-project.org/. Accessed on: Jan, 2021.

Reimann C.R., Bahlburg H., Kooijman E., Berndt J., Gerdes A., Carlotto V., López S. 2010. Geodynamic evolution of the early Paleozoic Western Gondwana margin 14°-17°S reflected by the detritus of the Devonian and Ordovician basins of southern Peru and northern Bolivia. *Gondwana Research*, **18**(2-3):370-384. https://doi.org/10.1016/j.gr.2010.02.002

Rezende de Oliveira J., Aguilar de Sousa M.Z., Salina Ruiz A., Matos Salinas G.R. 2017. Granulito Uyarani - Uma janela estrutural Pré-Cambriana no Altiplano Boliviano: Petrogênese e significado tectônico. *Geologia USP. Série Científica*, **17**(2):223-245. https://doi.org/10.11606/issn.2316-9095.v17-385

Servicio Geológico de Bolivia (GEOBOL). 1994. *Carta geológica de Bolivia.* Hoja Chulumani (6044). Escala 1:100,000. Bolivia: GEOBOL.

Servicio Geológico de Bolivia (GEOBOL). 1995. *Carta geológica de Bolivia.* Hoja Sapahaqui (6043). Escala 1:100,000. Bolivia: GEOBOL.

Servicio Geológico de Bolivia (GEOBOL). 1997. *Carta geológica de Bolivia.* Hoja Inquisivi (6143). Escala 1:100,000. Bolivia: GEOBOL.

Servicio Geológico de Bolivia (GEOBOL). 2013. *Carta geológica de Bolivia.* Hoja Challana (5946). Escala 1:100,000. Bolivia: GEOBOL.

Souza de Alvarenga C.J., Boggiani P.C., Babinski M., Dardenne M.A., Figueiredo M.F., Dantas E.L., Uhlein A., Santos R.V., Sial A.N., Trompette R. 2011. Glacially influenced sedimentation of the Puga Formation, Cuiabá Group and Jacadigo Group, and associated carbonates of the Araras and Corumbá groups, Paraguay Belt, Brazil. *Journal of the Geological Society*, **36**(1):487-497. https://doi.org/10.1144/M36.45

Suárez-Soruco R. 1992. El Paleozoico Inferior de Bolivia y Perú. *In*: Gutiérrez M.J.G., Saavedra J., Rábano I. (eds.). *El Paleozoico Inferior de Ibero-América*. Badajoz, España, Universidad de Extremadura, p. 225-239.

Suárez-Soruco R. 2000. Compendio de Geologia de Bolivia. *Revista Técnica de Yacimientos Petrolíferos Fiscales de Bolivia*, **18**(1-2).

Vasconcelos B.R. 2018. *Proveniência sedimentar do Grupo Cuiabá na faixa Paraguai Meridional.* Tese de Doutorado, Universidade de Brasília, Brasília.

Voges A. 1962. *Geología y yacimientos metalíferos de la región de Oruro.* Misión Geológica Alemana en Bolivia (MGAB).

Wiedenbeck M., Allé P., Corfu F., Griffin W.L., Meier M., Oberli F., Von Quadt A., Roddick J.C., Spiegel W. 1995. Three natural zircon standards for U-Th-Pb, Lu-Hf, trace-element and REE analyses. *Geostandards Newsletter*, **19**(1):1-23. https://doi.org/10.1111/j.1751-908X.1995.tb00147.x